

Possible Routes to Frictionless Transport of Electronic Fluids in High-Temperature Superconductors

Zotin K.-H. Chu

3/F, 24, 260th. Lane, First Section, Muja Road, Taipei, Taiwan 116, China and
P.O. Box 39, Distribution Unit, Xihong Road, Urumqi 830000, China

Abstract

Electric-field-driven transport of electronic fluids in metallic glasses as well as three-dimensional amorphous superconductors are investigated by using the verified approach which has been successfully adopted to study the critical transport of glassy solid helium in very low temperature environment. The critical temperatures related to the nearly frictionless transport of electronic fluids were found to be directly relevant to the superconducting temperature of amorphous superconductors after selecting specific activation energies. Our results imply that optimal shear-thinning is an effective way to reach high-temperature charged superfluidity or superconductivity.

Key words Transport, critical temperature.

PACS 74.81.Bd, 74.25.Sv, 74.70.Ad, 72.15.Cz, 74.20.Mn, 72.10.Bg, 71.23.Cq, 64.70.pe,

1 Introduction

Analogies between superconductivity (charged superfluidity) and superfluidity in liquid [1-2] and solid helium (either supersolid [3] or superglass [4-6]) has been noted by some researchers. The particles (charged electrons as well as atoms) in a superfluid are in the same quantum state, so they move coherently and result in dissipationless mass flow. Quite recently a glassy state of supersolid helium (solid ^4He : ability to flow without resistance) has been reported [5]. We have made some contributions to the possible transport of glassy solid ^4He in confined domain under rather low temperature environment (cf. Ref. 6 for the comparison with available relevant experiments). Our present interest is to borrow the above mentioned analogy to investigate the nearly frictionless states for transport of the electronic liquid (presumed to be glassy or amorphous) in amorphous superconductors [7-10] which is closely related to charged frictionless or superfluidity states. The approach adopted in [6] (considering transport of glassy fluids) will be extended by varying the forcing to be an electric field in this paper.

Note that one prominent difference between the fluid transport in microdomain and those in macrodomain is the strong fluid-wall interactions observed in microconduits. For example, as the microconduit size decreases, the surface-to-volume ratio increases. Therefore, various properties of the walls, such as surface roughness, greatly affect the fluid motions in microconduits. In this paper, we adopt the verified Eyring model [6,11-13] to study the nearly frictionless trans-

port of (glassy) electronic fluids within corrugated microannuli. Eyring model treats transport of shear-thinning (which means once material is subjected to high shear rates then the viscosity diminishes with increasing shear rate) matter quite successfully [6,11-13]. To obtain the law of shear-thinning fluids for explaining the too rapid annealing at the earliest time, because the relaxation at the beginning was steeper than could be explained by the bimolecular law, a hyperbolic sine law between the shear (strain) rate : $\dot{\gamma}$ and (large) shear stress : τ was proposed and the close agreement with experimental data was obtained [11-13]. This model has sound physical foundation from the thermal activation process (Eyring [12] already considered a kind of (quantum) tunneling which relates to the matter rearranging by surmounting a potential energy barrier). With this model we can associate the (shear-thinning) electronic fluid with the momentum transfer between neighboring clusters on the microscopic scale and reveals the detailed interaction in the relaxation of flow with dissipation (the momentum transfer depends on the activation shear volume, which is associated with the center distance between (charged) particles and is proportional to $k_B T / \tau_0$ (T is temperature in Kelvin, and τ_0 a constant with the dimension of stress)). Thus, this model could be applied to study transport of (shear-thinning as well as amorphous or glassy) electronic fluids in microdomain which is of particular interest to researchers in condensed matter physics (considering amorphous superconductors [7-10]). We select the microannular geometry as it is more relevant to the experimental environment considering the measuring conductivity of samples of amorphous superconductors [7-10] (transport of shell-like electronic fluids).

To consider the more realistic but complicated boundary conditions in the walls of microannulus, however, we will use the boundary perturbation technique [13-14] to handle the presumed wavy-roughness along the walls of microannuli. To obtain the analytical and approximate solutions, here, the roughness is only introduced in the radial or transverse direction. The relevant boundary conditions along the wavy-rough surfaces will be prescribed below. We shall describe our approach after this section : Introduction with the focus upon the boundary perturbation method. The expression of the electric-field-driven volume flow rate of the glassy (or amorphous) electronic fluid is then demonstrated at the end. We noticed that the conductivity measurements reported in [9] and [10] are primary in Mg-based and $\text{Fe}_x\text{Ni}_{1-x}$ -based metallic glasses. Finally, we will illustrate our results into four figures and give discussions therein. Our results show that some specific activation energies and activation volumes are crucial to the nearly frictionless states of the transport of the electronic fluids at rather low temperature regime. The good qualitative as well as quantitative (e.g., critical temperature or T_c) comparison with experiments confirms our approaches. Our results imply that optimal shear-thinning is an effective way to reach high-temperature charged superfluidity or superconductivity.

2 Formulations

Researchers have been interested in the question of how amorphous material responds to an external mechanical load. External loads cause (electronic) liquids to flow, in Newtonian or various types of non-Newtonian flows. Glassy materials, composed of polymers, metals, or ceramics, can deform under mechanical loads, and the nature of the response to loads often dictates the choice of material in various industrial applications. The nature of all of these responses depends on both the temperature and loading rate. As described by Eyring [12], mechanical loading lowers energy barriers, thus facilitating progress over the barrier by random thermal fluctuations. The Eyring model approximates the loading dependence of the barrier height as linear. The Eyring model, with this linear barrier height dependence on load, has been used over a large fraction of the last century to describe the response of a wide range of systems and underlies modern approaches to sheared glasses [11-12]. To the best knowledge of the author, the simplest model that makes a prediction for the rate and temperature dependence of shear yielding is the rate-state Eyring model of stress-biased thermal activation [11-12]. Structural rearrangement is associated with a single energy barrier E that is lowered or raised linearly by an applied stress σ .

$$R_{\pm} = \nu_0 \exp[-E/(k_B T)] \exp[\pm \sigma V^*/(k_B T)],$$

where k_B is the Boltzmann constant, ν_0 is an attempt frequency and V^* is a constant called the activation volume. In glasses, the transition rates are negligible at zero stress. Thus, at finite stress one needs to consider only the rate R_+ of transitions in the direction aided by stress.

The linear dependence will always correctly describe small changes in the barrier height, since it is simply the first term in the Taylor expansion of the barrier height as a function of load. It is thus appropriate when the barrier height changes only slightly before the system escapes the local energy minimum. This situation occurs at higher temperatures; for example, Newtonian flow is obtained in the Eyring model in the limit where the system experiences only small changes in the barrier height before thermally escaping the energy minimum. As the temperature decreases, larger changes in the barrier height occur before the system escapes the energy minimum (giving rise to, for example, non-Newtonian flow). In this regime, the linear dependence is not necessarily appropriate, and can lead to inaccurate modeling. To be precise, at low shear rates ($\dot{\gamma} \leq \dot{\gamma}_c$), the system behaves as a power law shear-thinning material while, at high shear rates, the stress varies affinely with the shear rate. These two regimes correspond to two stable branches of stationary states, for which data obtained by imposing either σ or $\dot{\gamma}$ exactly superpose. The transition from the lower branch to the higher branch occurs through a stable hysteretic loop in a stress-controlled experiment.

The motion (of composite particles) is represented in the configuration space; on the potential surface the stable particles are in the valleys, which are connected by a pass that leads through

the saddle point. A (composite) particle at the saddle point is in the transition (activated) state. Under the action of an applied stress the forward velocity of a flow unit is the net number of times it moves forward, multiplied by the distance it jumps. Eyring proposed a specific microscopic model of the amorphous structure and a mechanism of deformation kinetics [11-12]. With reference to this idea, this mechanism results in a (shear) strain rate given by

$$\dot{\gamma} = 2 \frac{V_h}{V_m} \frac{k_B T}{h} \exp\left(\frac{-\Delta E}{k_B T}\right) \sinh\left(\frac{V_h \tau}{2k_B T}\right) \quad (1)$$

where

$$V_h = \lambda_2 \lambda_3 \lambda, \quad V_m = \lambda_2 \lambda_3 \lambda_1,$$

λ_1 is the perpendicular distance between two neighboring layers of (composite) particles sliding past each other, λ is the average distance between equilibrium positions in the direction of motion, λ_2 is the distance between neighboring (composite) particles in this same direction (which may or may not equal λ), λ_3 is the (composite) particle to (composite) particle distance in the plane normal to the direction of motion, and τ is the local applied stress, ΔE is the activation energy, h is the Planck constant, k_B is the Boltzmann constant, T is the temperature, V_h is the activation volume for the microscopic event [12]. The deformation kinetics of the chain (composite particles) is envisaged as the propagation of kinks in the particles into available holes. In order for the motion of the kink to result in a flow, it must be raised (energised) into the activated state and pass over the saddle point. This was the earliest microscopic theory of yield behaviour in amorphous materials, and Eyring presented a theoretical framework which formed the basis of many subsequent considerations.

Solving Eqn. (1) for τ , one obtains:

$$\tau = \frac{2k_B T}{V_h} \sinh^{-1}\left(\frac{\dot{\gamma}}{B}\right), \quad (2)$$

which in the limit of small $(\dot{\gamma}/B)$ reduces to Newton's law for viscous deformation kinetics.

We shall consider a steady transport of the glassy (or amorphous) electronic fluids in a wavy-rough microannulus of r_1 (mean-averaged inner radius) with the inner interface being a fixed wavy-rough surface : $r = r_1 + \epsilon \sin(k\theta + \beta)$ and r_2 (mean-averaged outer radius) with the outer interface being a fixed wavy-rough surface : $r = r_2 + \epsilon \sin(k\theta)$, where ϵ is the amplitude of the (wavy) roughness, β is the phase shift between two boundaries, and the roughness wave number : $k = 2\pi/L$ (L is the wavelength of the surface modulation in transverse direction).

Firstly, this amorphous fluid [6,12-13] can be expressed as $\dot{\gamma} = \dot{\gamma}_0 \sinh(\tau/\tau_0)$, where $\dot{\gamma}$ is the shear rate, τ is the shear stress, and $\dot{\gamma}_0 \equiv B$ is a function of temperature with the dimension of the shear rate. In fact, the force balance gives the shear stress at a radius r as $\tau = -[r \delta(\rho_e E_z)]/2$, where τ is the shear stress along the boundaries of a control volume in the flow direction (the same direction as E_z which (the only electric field) is presumed to be a constant or uniform), ρ_e is the net charge density, $|\delta(\rho_e E_z)|$ is the net electric force along the transport (or tube-axis

: z -axis) direction.

Introducing $\chi = -(r_2/2\tau_0)\delta(\rho_e E_z)$ then we have $\dot{\gamma} = \dot{\gamma}_0 \sinh(\chi r/r_2)$. As $\dot{\gamma} = -du/dr$ (u is the velocity of the (electronic) fluid transport in the longitudinal (z -)direction of the microannulus), after integration, we obtain

$$u = u_s + \frac{\dot{\gamma}_0 r_2}{\chi} [\cosh \chi - \cosh(\frac{\chi r}{r_2})], \quad (3)$$

here, u_s is the velocity over the (inner or outer) surface of the microannulus, which is determined by the boundary condition. We noticed that a general boundary condition [13] was proposed for transport over an interface as

$$\Delta u = L_s^0 \dot{\gamma} (1 - \frac{\dot{\gamma}}{\dot{\gamma}_c})^{-1/2}, \quad (4)$$

where Δu is the velocity jump over the interface, L_s^0 is a constant slip length, $\dot{\gamma}_c$ is the critical shear rate at which the slip length diverges. The value of $\dot{\gamma}_c$ is a function of the corrugation of interfacial energy.

With the boundary condition from [13], we can derive the velocity fields and electric-field-driven volume flow rates along the wavy-rough microannulus below using the verified boundary perturbation technique [6,13-14]. The wavy boundaries are prescribed as $r = r_2 + \epsilon \sin(k\theta)$ and $r = r_1 + \epsilon \sin(k\theta + \beta)$ and the presumed steady transport is along the z -direction (microannulus-axis direction).

Along the outer boundary (the same treatment below could also be applied to the inner boundary), we have $\dot{\gamma} = (du)/(dn)|_{\text{on surface}}$. Here, n means the normal. Let u be expanded in ϵ : $u = u_0 + \epsilon u_1 + \epsilon^2 u_2 + \dots$, and on the boundary, we expand $u(r_0 + \epsilon dr, \theta (= \theta_0))$ into

$$\begin{aligned} u(r, \theta)|_{(r_0 + \epsilon dr, \theta_0)} &= u(r_0, \theta) + \epsilon [dr u_r(r_0, \theta)] + \epsilon^2 [\frac{dr^2}{2} u_{rr}(r_0, \theta)] + \dots = \\ \{u_{slip} + \frac{\dot{\gamma} r_2}{\chi} [\cosh \chi - \cosh(\frac{\chi r}{r_2})]\} &|_{\text{on surface}}, \quad r_0 \equiv r_1, r_2; \end{aligned} \quad (5)$$

where

$$u_{slip}|_{\text{on surface}} = L_s^0 \dot{\gamma} [(1 - \frac{\dot{\gamma}}{\dot{\gamma}_c})^{-1/2}]|_{\text{on surface}}. \quad (6)$$

Now, on the outer interface (cf. [13-14])

$$\dot{\gamma} = \frac{du}{dn} = \nabla u \cdot \frac{\nabla(r - r_2 - \epsilon \sin(k\theta))}{|\nabla(r - r_2 - \epsilon \sin(k\theta))|}. \quad (7)$$

Considering $L_s^0 \sim r_1, r_2 \gg \epsilon$ case, we also presume $\sinh \chi \ll \dot{\gamma}_c/\dot{\gamma}_0$. With equations (1) and (5), using the definition of $\dot{\gamma}$, we can derive the velocity field (u) up to the second order : $u(r, \theta) = -(r_2 \dot{\gamma}_0/\chi) \{ \cosh(\chi r/r_2) - \cosh \chi [1 + \epsilon^2 \chi^2 \sin^2(k\theta)/(2r_2^2)] + \epsilon \chi \sinh \chi \sin(k\theta)/r_2 \} + u_{slip}|_{r=r_2 + \epsilon \sin(k\theta)}$. The key point is to firstly obtain the slip velocity along the boundaries or surfaces. After lengthy mathematical manipulations, we obtain the velocity fields (up to the second order) and then

we can integrate them with respect to the cross-section to get the volume flow rate (Q , also up to the second order here) : $Q = \int_0^{\theta_p} \int_{r_1+\epsilon \sin(k\theta+\beta)}^{r_2+\epsilon \sin(k\theta)} u(r, \theta) r dr d\theta = Q_{slip} + \epsilon Q_{p1} + \epsilon^2 Q_{p2}$. In fact, the approximately (up to the second order) net electric-field-driven volume flow rate reads $Q \equiv Q_{out} - Q_{in}$ which is the flow within the outer (larger) wall : Q_{out} without the contributions from the flow within the inner (smaller) wall Q_{in} :

$$\begin{aligned}
Q = & \pi \dot{\gamma}_0 \{ L_s^0 (r_2^2 - r_1^2) \sinh \chi (1 - \frac{\sinh \chi}{\dot{\gamma}_c / \dot{\gamma}_0})^{-1/2} + \frac{r_2}{\chi} [(r_2^2 - r_1^2) \cosh \chi - \frac{2}{\chi} (r_2^2 \sinh \chi - \\
& r_1 r_2 \sinh(\chi \frac{r_1}{r_2}) + \frac{2r_2^2}{\chi^2} (\cosh \chi - \cosh(\chi \frac{r_1}{r_2}))] \} + \epsilon^2 \{ \pi \dot{\gamma}_0 [\chi \frac{\cosh \chi}{4} (r_2 - \frac{r_1^2}{r_2})] + \\
& \frac{\pi}{4} \dot{\gamma}_0 \sinh \chi (1 + \frac{\sinh \chi}{\dot{\gamma}_c / \dot{\gamma}_0}) (-k^2 + \chi^2) [1 - (\frac{r_1}{r_2})^2] + \frac{\pi}{2} [(u_{slip0} + \\
& \frac{\dot{\gamma}_0 r_2}{\chi} \cosh \chi) + \dot{\gamma}_0 r_2 (-\sinh \chi + \frac{\cosh \chi}{\chi}) + \dot{\gamma}_0 (r_1 \sinh(\chi \frac{r_1}{r_2}) - \frac{r_2}{\chi} \cosh(\chi \frac{r_1}{r_2}))] + \\
& \pi \dot{\gamma}_0 \{ [\sinh \chi + \chi \frac{\cosh \chi}{r_2} (1 + \frac{\sinh \chi}{\dot{\gamma}_c / \dot{\gamma}_0})] [r_2 - r_1 \cos \beta] \} + \\
& \frac{\pi}{4} \chi^2 \dot{\gamma}_0 \frac{\cosh \chi}{\dot{\gamma}_c / \dot{\gamma}_0} [1 - (\frac{r_1}{r_2})^2] \cosh \chi. \tag{8}
\end{aligned}$$

Here,

$$u_{slip0} = L_s^0 \dot{\gamma}_0 [\sinh \chi (1 - \frac{\sinh \chi}{\dot{\gamma}_c / \dot{\gamma}_0})^{-1/2}]. \tag{9}$$

3 Results and Discussions

We firstly check the roughness effect upon the shearing characteristics because there are no available experimental data and numerical simulations for the same geometric configuration (microscopic annuli with wavy corrugations in transverse direction). With a series of forcings (due to imposed electric fields) : $\chi \equiv r_2 [-\delta(\rho_e E_z)] / (2\tau_0)$, we can determine the enhanced shear rates ($d\gamma/dt$) due to forcings. From equation (7), we have (up to the first order)

$$\frac{d\gamma}{dt} = \frac{d\gamma_0}{dt} [\sinh \chi + \epsilon \sin(k\theta) \frac{\chi}{r_2} \cosh \chi]. \tag{10}$$

Furthermore, if we select a (fixed) temperature, then from the expression of τ_0 , we can obtain the shear stress τ corresponding to above forcings (χ) :

$$\tau = \tau_0 \sinh^{-1} [\sinh(\chi) + \epsilon \sin(k\theta) \frac{\chi}{r_2} \cosh(\chi)]. \tag{11}$$

Note that, based on the absolute-reaction-rate Eyring model (of stress-biased thermal activation), structural rearrangement is associated with a single energy barrier (height) ΔE that is lowered or raised linearly by a (shear) yield stress τ . If the transition rate is proportional to the

plastic (shear) strain rate (with a constant ratio : C_0 ; $\dot{\gamma} = C_0 R_t$, R_t is the transition rate in the direction aided by stress), we have

$$\tau = 2\left[\frac{\Delta E}{V_h} + \frac{k_B T}{V_h} \ln\left(\frac{\dot{\gamma}}{C_0 \nu_0}\right)\right] \quad \text{if} \quad \frac{V_h \tau}{k_B T} \gg 1 \quad (12)$$

where ν_0 is an attempt frequency or transition rate, $C_0 \nu_0 \sim \dot{\gamma}_0 \exp(\Delta E/k_B T)$, or

$$\tau = 2\frac{k_B T}{V_h} \frac{\dot{\gamma}}{C_0 \nu_0} \exp(\Delta E/k_B T) \quad \text{if} \quad \frac{V_h \tau}{k_B T} \ll 1. \quad (13)$$

The nonlinear character only manifests itself when the magnitude of the applied stress times the activation volume becomes comparable or greater in magnitude than the thermal vibrational energy.

The following figures are for our primary interest : Higher (electric) conductivity or lower viscosity which means rather low resistance of the electric-field-driven transport of amorphous electron liquid. This can be manifested from equation (8) for the net transport $Q (\propto \sinh \chi)$. We have the average velocity (for charge carriers) : $\bar{v} = Q/A_m$ with A_m being the effective area. After this, we then have the electric flux : $\rho_e \bar{v} = |\mathbf{J}|$ which conventionally equals to σE_z where σ is the electrical conductivity. Thus we can obtain the electrical resistance $\rho_R = 1/\sigma$. The latter is directly relevant to the frictional resistance or shear stress along the tube wall considering the balancing of the driven electrical force when the transport is finally steady or fully developed. This can be evidenced easily once χ is small then we have $\rho_R^{-1} \propto \bar{v} \propto \sinh \chi \sim \chi \propto |-\delta(\rho_e E_z)|$. Fig. 1 shows that there will be nearly frictionless or almost zero-resistance states if we select the activation energy to be 10^{-22} J ~ 0.001 eV. We can observe a sudden drop of the resistance (frictional or shear stress) around 3 orders of magnitude at $T = 0.12^\circ\text{K}$ ($V_h \approx 10^{-24}\text{m}^3$). It means there is a rather high electrical conductivity (or very low electrical resistivity) around this temperature for the material parameters selected. The qualitative as well as quantitative similarity are that this critical temperature (T_c phenomenon) resembles that found in amorphous superconductor $\text{Mg}_{70}\text{Zn}_{30}$ (cf. [9]).

Similarly, Fig. 2 shows that there are almost zero-resistance states if we select the activation energy to be 10^{-22} J ~ 0.001 eV. We can observe a sudden drop of the resistance (frictional or shear stress) around 3 orders of magnitude at $T = 1.9^\circ\text{K}$ ($V_h \approx 10^{-23}\text{m}^3$). It means there is a rather high electrical conductivity (or very low electrical resistivity) around this temperature for the material parameters selected. The qualitative as well as quantitative similarity are that this critical temperature (T_c phenomenon) resembles that found in amorphous superconductor $\text{Fe}_x\text{Ni}_{1-x}\text{Zr}_2$ ($x \sim 0.4$; cf. Table 1 in [10]).

To verify more of our approach, we demonstrate that if we select the activation energy to be 10^{-22} J ~ 0.001 eV we can then observe a sudden drop of the resistance (frictional or shear stress) around 1 order of magnitude at $T = 4.56^\circ\text{K}$ ($V_h \approx 10^{-23}\text{m}^3$). It means there is a rather high electrical conductivity (or very low electrical resistivity) around this temperature for the

material parameters selected. The qualitative as well as quantitative similarity are that this critical temperature (T_c phenomenon) resembles that found in amorphous superconductor $\text{Zr}_{75}\text{Rh}_{25}$ (cf. Fig. 1 (a) and Fig. 2 for the zero (magnetic) field case in [8]).

Furthermore, Fig. 4 illustrates that there are almost zero-resistance states if we select the activation energy to be 3.5×10^{-19} J. We can observe a starting (sudden) drop of the resistance (frictional or shear stress) at $T \sim 164^\circ\text{K}$ ($V_h \approx 10^{-20}\text{m}^3$) around 3 orders of magnitude and below $T = 80^\circ\text{K}$. This also demonstrates that there is a rather high electrical conductivity (or very low electrical resistivity) around this temperature for the material parameters selected. The qualitative as well as quantitative similarity are that this critical temperature (T_c phenomenon) resembles that found in amorphous high- T_c superconductor $\text{Hg}_{1-x}\text{Pb}_x\text{Ba}_2\text{Ca}_2\text{Cu}_3\text{O}_{8+\delta}$ [$\text{Hg}(x\text{Pb})$ 1:2:2:3] [15].

To give a brief summary, we already used the verified approach by borrowing the analogy from the successful application to the study of the almost frictionless transport of glassy solid helium to obtain the critical transport of electric-field-driven electronic fluids in metallic glasses as well as amorphous (bulk) superconductors. The critical temperatures we found after tuning of the material parameters resemble qualitatively as well as quantitatively those superconducting temperatures reported before in (3D) amorphous superconductors. Our results show that effective shear-thinning is an important way to reach high-temperature charged superfluidity or superconductivity. We shall investigate other interesting issues [5,16] in the coming future.

References

- [1] J. Bardeen, Phys. Rev. Lett. **1**, 399 (1958).
- [2] R. Friedberg and T.D. Lee, J. Superconductivity Novel Magnetism **19**, 277 (2006).
- [3] P.W. Anderson, Nature Phys. **3**, 160 (2007) [cond-mat/0606429, (2006)].
- [4] A.F. Andreev, JETP Lett. **85**, 585 (2007).
- [5] J. Saunders, Science **324**, 601 (2009).
- [6] Z.K.-H. Chu, arXiv:0809.4085 (2008).
- [7] W.L. Johnson and C.C. Tsuei, Phys. Rev. B **13**, 4827 (1976).
- [8] W.L. Johnson, C.C. Tsuei and P. Chaudhari, Phys. Rev. B **17**, 2884 (1978).
- [9] R. Richter, D.V. Baxter and J.O. Strom-Olsen, Phys. Rev. B **38**, 10421 (1988).
- [10] Z. Altounian, S.V. Dantu and M. Dikeakos, Phys. Rev. B **49**, 8621 (1994).
- [11] F.W. Cagle, Jr. and H. Eyring, J. Appl. Phys. **22**, 771 (1951).

- [12] H. Eyring, J. Chem. Phys. **4**, 283 (1936).
F.H. Ree, T.S. Ree, T. Ree and H. Eyring, Adv. Chem. Phys. **4**, 1 (1962).
- [13] Z. K.-H. Chu, arXiv:0707.2828 (2007). Z. K.-H. Chu, Ann. Phys. (Berlin) **17**, 343 (2008).
- [14] W. K.-H. Chu, ZAMP **47**, 591 (1996). W. K.-H. Chu, ZAMM **76**, 363 (1996).
- [15] L. Gao, *et al.* Phys. Rev. B **50**, 4260 (1994).
- [16] I. Morgenstern, K.A. Müller and J.G. Bednorz, Z. Phys. B-Condensed Matter **69**, 3347 (1987). K.A. Müller, M. Takashige and J.G. Bednorz, Phys. Rev. Lett. **58**, 1143 (1987).

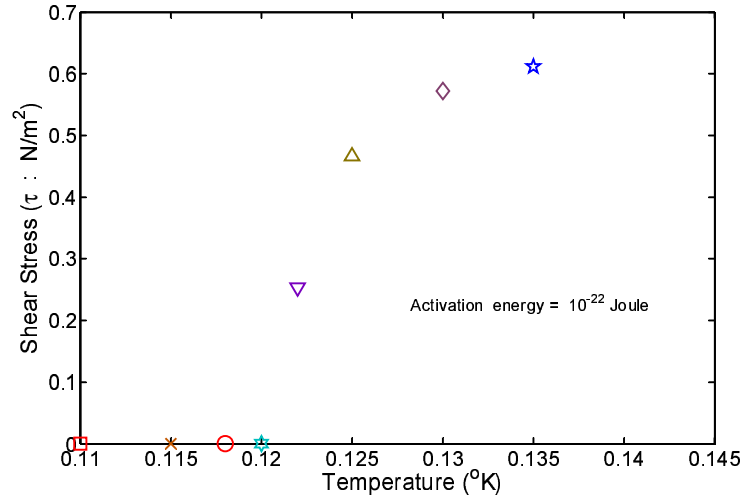


Fig. 1. Calculated (shear) stresses or resistance using an activation energy 10^{-22} J or ~ 0.001 eV. There is a sharp decrease of shear stress around $T \sim 0.12^{\circ}\text{K}$. Around 0.12 K, the electric-field-driven transport of (glassy) electronic fluid is nearly frictionless. This critical temperature resembles that found in amorphous superconductor $\text{Mg}_{70}\text{Zn}_{30}$ (cf. [9]).

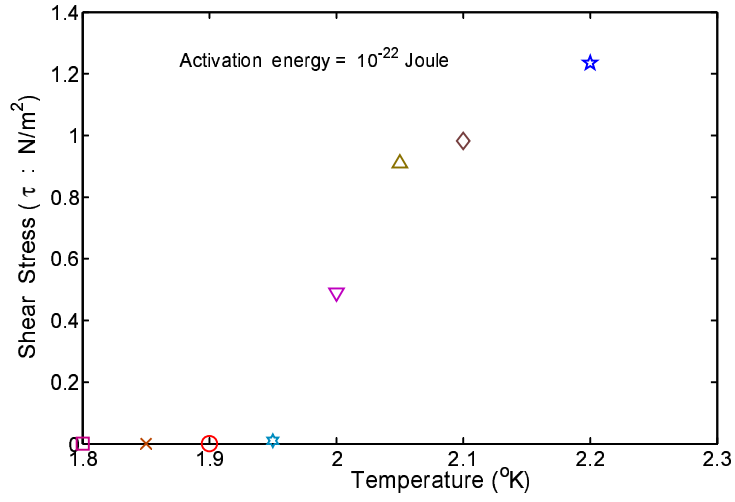


Fig. 2 Calculated (shear) stresses or resistance using an activation energy 10^{-22} J or ~ 0.001 eV. There is a sharp decrease of shear stress around $T \sim 1.9^\circ\text{K}$. Around 1.9 K, the electric-field-driven transport of (glassy) electronic fluid is nearly frictionless. This critical temperature resembles that found in amorphous superconductor $\text{Fe}_x\text{Ni}_{1-x}\text{Zr}_2$ (cf. Table 1 in [10] : $x \sim 0.4$).

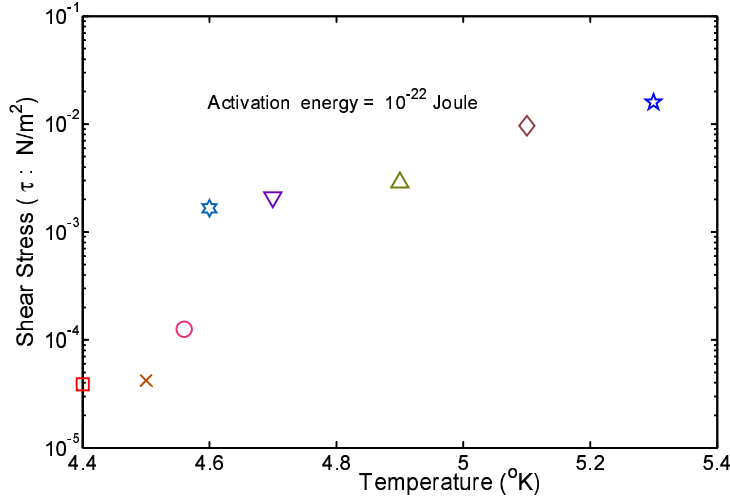


Fig. 3 Calculated (shear) stresses or resistance using an activation energy 10^{-22} J or ~ 0.001 eV. There is a sharp decrease of shear stress around $T \sim 4.56^\circ\text{K}$. Around 4.5 K, the electric-field-driven transport of (glassy) electronic fluid is nearly frictionless. This critical temperature resembles that found in amorphous superconductor $\text{Zr}_{75}\text{Rh}_{25}$ (cf. Fig. 1 (a) and Fig. 2 in [8] : the zero (magnetic) field case).

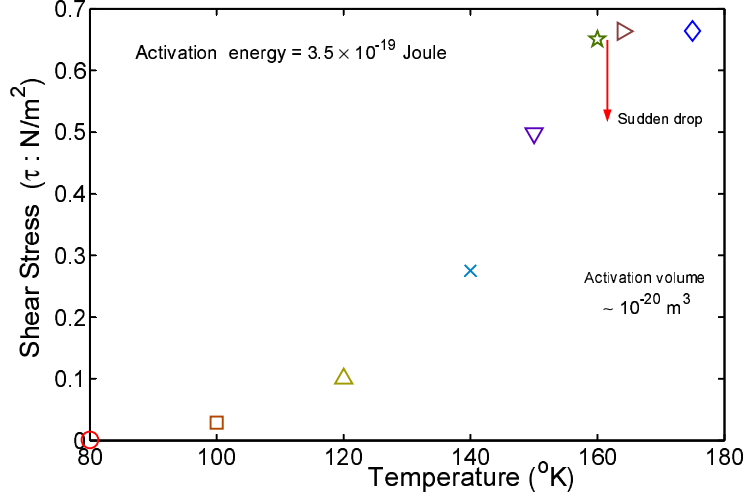


Fig. 4 Calculated (shear) stresses or resistance using an activation energy 3.5×10^{-19} J. There is a sharp decrease of shear stress starting from around $T \sim 164^\circ\text{K}$. Below around 80 K, the electric-field-driven transport of (glassy) electronic fluid is nearly frictionless. This critical temperature resembles that found in amorphous high-temperature superconductor $\text{Hg}_{1-x}\text{Pb}_x\text{Ba}_2\text{Ca}_2\text{Cu}_3\text{O}_{8+\delta}$ [Hg(x Pb) 1:2:2:3] [15].